

**Derivation of  
Voltage and Current Transfer Functions for  
Multiconductor Transmission Lines**

**Mike Riddle  
Sasan Ardalan  
John Suh**

**1988**

**Center for Communications and Signal Processing  
Dept. of Electrical and Computer Engineering  
North Carolina State University  
Raleigh, NC 27650-7914**

## **Abstract**

A set of new and compact equations are derived for solving a system of multiconductor transmission lines with arbitrary source and load termination networks. The derivations are based on defining the reflection coefficient matrix for multiconductor transmission lines. Expressions for the voltage and current transfer functions are derived. For the two conductor case, the equations reduce to well known results. The expressions are very suitable for straight forward coding on a computer. The validity of the derived equations is checked with published experimental and computer models for three and four conductor transmission line systems.

## Table of Contents

1. Introduction.....	3
2. Derivation of Muticonductor Transfer Functions.....	3
3. Two Conductor Transmission Line System.....	10
4. Summary of Derived Results.....	12
5. Comparison with Published Experimental and Computer Results .....	13
5.1 Reduction of Inductive Coupling by Reducing Cross-section.....	13
5.2 Four Conductor Transmission Line System.....	15
5.3 Three Conductor Coupling.....	17
6. Conclusions.....	21
7. References .....	21

## 1. Introduction

The study of coupling between wires in multiconductor systems is important in many communication systems. These include near-end and far-end crosstalk in the subscriber loop in telephone networks, coupling to and from twisted wire pairs in high speed Local Area Networks (LANs), the prediction of voltage distribution in poly-phase distribution line systems in power line communications, and the prediction of crosstalk noise due to high speed switching in printed circuit boards [6-17].

Previously expressions have been derived for solving multiconductor transmission line systems, for example in [3] and [4]. These expressions are not compact nor do they easily reduce directly to familiar two conductor equations [1]. In this paper a set of compact equations are derived for solving a system of multiconductor transmission lines with arbitrary source and load terminations. Also expressions for the voltage and current transfer functions in terms of the reflection coefficient at the load are derived. In the derivation, the reflection coefficient matrix is defined and the voltage and current vectors and input impedance matrix are derived in terms of the reflection coefficient matrix at the load.

The equations derived in this paper were coded in a computer program and used to solve a number of multiconductor transmission line systems. Published experimental and computer model predictions for these systems were available in the excellent work in [5] and [6].

Further comparisons between the derived multiconductor equations and measurements from poly-phase power distribution lines, under a variety of loading conditions, is presented in [16] and [17].

## 2. Derivation of Multiconductor Transfer Functions

Consider a transmission line system of  $n+1$  conductors driven by an arbitrary source network and terminated by an arbitrary load network as shown in Figure 1.

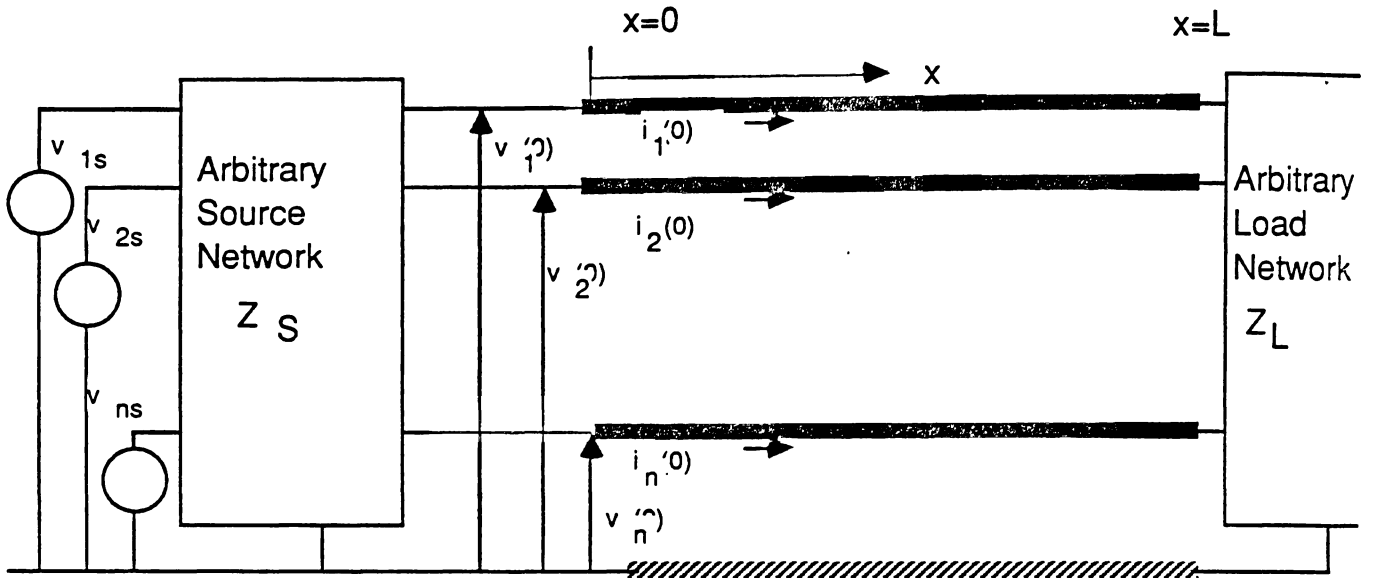


Figure 1. Multiconductor Transmission Line Configuration

We can collect the conductor voltages and currents at any point along the line,  $x$ , in vectors as follows,

$$\mathbf{V}(x) = [ v_1(x), v_2(x), \dots, v_n(x) ]^T \quad (1)$$

$$\mathbf{I}(x) = [ i_1(x), i_2(x), \dots, i_n(x) ]^T \quad (2)$$

Under suitable conditions, a transmission line system can be characterized by its per-unit parameters. Consider the three conductor case shown in Figure 2.

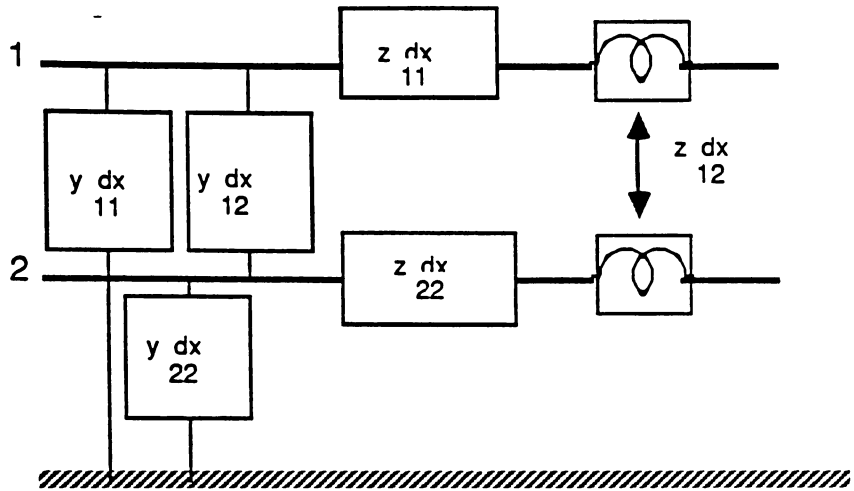


Figure 2. Three conductor per unit parameters.

We define the impedance per unit length matrix as,

$$Z = \begin{bmatrix} z_{11} & z_{12} \\ z_{12} & z_{22} \end{bmatrix} \quad (3)$$

and the admittance per unit length matrix as,

$$Y = \begin{bmatrix} y_{11} + y_{12} & -y_{12} \\ -y_{12} & y_{22} + y_{12} \end{bmatrix} \quad (4)$$

For general  $n+1$  conductors,

$$Z = \begin{bmatrix} z_{11} & z_{12} & \dots & z_{1n} \\ z_{12} & z_{22} & \dots & z_{2n} \\ \dots & \dots & \dots & \dots \\ z_{1n} & \dots & \dots & z_{nn} \end{bmatrix} \quad (5)$$

and,

$$Y = \begin{bmatrix} y_{11} + y_{12} + \dots + y_{1n} & -y_{12} & \dots & -y_{1n} \\ -y_{12} & y_{22} + y_{12} + \dots + y_{2n} & \dots & -y_{2n} \\ \dots & \dots & \dots & \dots \\ -y_{1n} & \dots & -y_{(n-1)n} & y_{nn} + y_{1n} + \dots + y_{(n-1)n} \end{bmatrix} \quad (6)$$

The vector differential equations for the general multiconductor transmission line can be written [1,2,3],

$$\frac{\partial V(x)}{\partial x} = -Z I(x) \quad (7)$$

$$\frac{\partial I(x)}{\partial x} = -Y V(x) \quad (8)$$

Solutions to the differential equations are [1,2,3],

$$V(x) = e^{-\gamma x} V_w^+ + e^{+\gamma x} V_w^- \quad (9)$$

and

$$I(x) = e^{-\gamma x} I_w^+ - e^{+\gamma x} I_w^- \quad (10)$$

In the above equations we have defined the propagation matrix

$$\gamma^2 = ZY \quad (11)$$

In (9)  $V_w^+$  is the incident vector voltage at  $x=0$ , or at the source boundary  $V_w^-$  is the reflected vector voltage at the source boundary. Similarly for  $I_w^+$  and  $I_w^-$ . Now, define the reflection coefficient at any point  $x$ ,  $\Gamma(x)$ ,

$$V_w^-(x) = \Gamma(x)V_w^+(x) \quad (12a)$$

$$\Gamma(x)e^{-\gamma x}V_w^+ = e^{\gamma x}V_w^- \quad (12b)$$

Or,

$$V_w^- = e^{-\gamma x}\Gamma(x)e^{-\gamma x}V_w^+ \quad (13)$$

Clearly,

$$V_w^- = \Gamma(0) V_w^+ \quad (14)$$

where  $\Gamma(0)$  is the reflection coefficient at the source boundary.

In deriving (9), a solution for the differential equations was,

$$V^+(x) = e^{-\gamma x}V_w^+ \quad (15)$$

By taking the derivative of (15) with respect to  $x$  and using (7) we can relate the forward travelling voltage vector and current,

$$I_w^+(x) = Y_0 e^{-\gamma x}V_w^+ \quad (16)$$

where we have defined the characteristic admittance matrix,



$$Y_0 = Z^{-1}\gamma \quad (17)$$

Define the input impedance at any point  $x$ ,

$$V(x) = Z_{in}(x)I(x) \quad (18)$$

Now, substitute for  $V(x)$  and  $I(x)$  based on (9) and (10) into (18). Next, eliminate  $I_w^+$  and  $I_w^-$  to obtain the following expression:

$$V_w^- = e^{-\gamma x} [Z_{in}(x)Y_0 + \Gamma]^{-1} [Z_{in}(x)Y_0 - \Gamma] e^{-\gamma x} V_w^+ \quad (19)$$

Compare (19) and (13) to obtain an expression for the reflection coefficient matrix,

$$\Gamma(x) = [Z_{in}(x)Y_0 + \Gamma]^{-1} [Z_{in}(x)Y_0 - \Gamma] \quad (20)$$

Similarly the input impedance at any point can be written in terms of the reflection coefficient,

$$Z_{in}(x) = [I + \Gamma(x)] [I - \Gamma(x)]^{-1} Y_0^{-1} \quad (21)$$

The reflection coefficient matrix at the load is,

$$\Gamma_L = \Gamma(L) = [Z_L Y_0 + \Gamma]^{-1} [Z_L Y_0 - \Gamma] \quad (22)$$

The boundary condition at the source is [3],

$$V(0) = V_s - Z_s I(0) \quad (23)$$

Hence,

$$V(0) = Z_{in}(0)[Z_s + Z_{in}(0)]^{-1} V_s \quad (24)$$

Write  $V(x)$  in terms of the incident voltage vector,

$$V(x) = [I + \Gamma(x)] e^{-\gamma x} V_w^+ \quad (25)$$

Let  $x=0$  in (25),

$$V_w^+ = [I + \Gamma(0)]^{-1} V(0) \quad (26)$$

To obtain an expression for  $V(x)$  only in terms of the source voltage  $V_s$  and source and load impedances, eliminate  $V_w^+$  between (25) and (26). Next substitute for  $V(0)$  from (24). After further substitutions as appropriate and some algebra we obtain,

$$V(x) = [I + e^{\gamma(x-L)} \Gamma_L e^{\gamma(x-L)}] e^{-\gamma x} [I - e^{-\gamma L} \Gamma_L e^{-\gamma L}]^{-1} Z_0 [Z_s + [I + e^{-\gamma L} \Gamma_L e^{-\gamma L}] [I - e^{-\gamma L} \Gamma_L e^{-\gamma L}]^{-1} Z_0]^{-1} V_s \quad (27)$$

Following the same procedure an expression for  $I(x)$  is found.

$$I(x) = Y_0 [I - e^{\gamma(x-L)} \Gamma_L e^{\gamma(x-L)}] e^{-\gamma x} [I - e^{-\gamma L} \Gamma_L e^{-\gamma L}]^{-1} Z_0 [Z_s + [I + e^{-\gamma L} \Gamma_L e^{-\gamma L}] [I - e^{-\gamma L} \Gamma_L e^{-\gamma L}]^{-1} Z_0]^{-1} V_s \quad (28)$$

An expression for the input impedance at any point  $x$  along the transmission line system can be obtained in terms of the reflection coefficient at the load.

$$Z_{in}(x) = [I + e^{\gamma(x-L)} \Gamma_L e^{\gamma(x-L)}] [I - e^{\gamma(x-L)} \Gamma_L e^{\gamma(x-L)}]^{-1} Y_0^{-1} \quad (29)$$

By evaluating (27) and (28) at  $x=0$ , we can obtain the voltage vector and current vector transfer functions for the transmission line system:

$$V(x) = [I + e^{\gamma(x-L)} \Gamma_L e^{\gamma(x-L)}] e^{-\gamma x} [I - e^{-\gamma L} \Gamma_L e^{-\gamma L}]^{-1} V(0) \quad (30)$$

$$I(x) = Y_0 [I - e^{\gamma(x-L)} \Gamma_L e^{\gamma(x-L)}] e^{-\gamma x} [I - e^{-\gamma L} \Gamma_L e^{-\gamma L}]^{-1} Z_0 I(0) \quad (31)$$

### 3. Two Conductor Transmission Line System

For two conductor transmission line systems the  $n \times n$  matrices in the above equations are scalars. In this case equations (27) and (28) reduce to the two conductor forms [1],

$$v(x) = \frac{v_s z_0}{z_0 + z_s} e^{-\gamma x} \frac{1 + \Gamma_L e^{-2\gamma(L-x)}}{1 - \Gamma_s \Gamma_L e^{-2\gamma L}} \quad (32)$$

and

$$i(x) = \frac{v_s}{z_0 + z_s} e^{-\gamma x} \frac{1 - \Gamma_L e^{-2\gamma(L-x)}}{1 - \Gamma_s \Gamma_L e^{-2\gamma L}} \quad (33)$$

In the above expressions the source and load reflection coefficients are,

$$\Gamma_L = \frac{z_L - z_0}{z_L + z_0} \quad (34)$$

and

$$\Gamma_s = \frac{z_s - z_0}{z_s + z_0} \quad (35)$$

The input impedance also reduces to,

$$Z_{in}(x) = \frac{1 + \Gamma_L e^{-2\gamma(L-x)}}{1 - \Gamma_L e^{-2\gamma(L-x)}} Z_0 \quad (36)$$

#### 4. Summary of Derived Results

The equations necessary to solve a system of multiconductor transmission lines with arbitrary source and load termination networks derived in this paper are summarized in the Tables below. In the tables,  $x$  is the distance from the source toward the load along the transmission lines. The length of the transmission line system is  $L$ .

Table I.
Summary of equations to solve a multiconductor transmission line system with arbitrary source and load termination networks.
Voltage vector $V(x) = [v_1(x), v_2(x), \dots, v_n(x)]^T$
Current vector $I(x) = [i_1(x), i_2(x), \dots, i_n(x)]^T$
Propagation matrix $\gamma^2 = ZY$
Characteristic admittance $Y_0 = Z^{-1}\gamma$
Reflection Coefficient at the Load $\Gamma_L = \Gamma(L) = [Z_L Y_0 + I]^{-1} [Z_L Y_0 - I]$
Conductor voltage at point $x$ along conductor $V(x) = [I + e^{\gamma(x-L)} \Gamma_L e^{\gamma(x-L)}] e^{-\gamma x} [I - e^{-\gamma L} \Gamma_L e^{-\gamma L}]^{-1} Z_0$ $[Z_s + [I + e^{-\gamma L} \Gamma_L e^{-\gamma L}] [I - e^{-\gamma L} \Gamma_L e^{-\gamma L}]^{-1} Z_0]^{-1} V_s$
Conductor current at point $x$ along conductor $I(x) = Y_0 [I - e^{\gamma(x-L)} \Gamma_L e^{\gamma(x-L)}] e^{-\gamma x} [I - e^{-\gamma L} \Gamma_L e^{-\gamma L}]^{-1} Z_0$ $[Z_s + [I + e^{-\gamma L} \Gamma_L e^{-\gamma L}] [I - e^{-\gamma L} \Gamma_L e^{-\gamma L}]^{-1} Z_0]^{-1} V_s$
Input Impedance at distance $x$ looking towards load $Z_{in}(x) = [I + e^{\gamma(x-L)} \Gamma_L e^{\gamma(x-L)}] [I - e^{\gamma(x-L)} \Gamma_L e^{\gamma(x-L)}]^{-1} Y_0^{-1}$

Table II.
<p style="text-align: center;">Voltage transfer function</p> $V(x) = [1 + e^{\gamma(x-L)} \Gamma_L e^{\gamma(x-L)}] e^{-\gamma x} [1 - e^{-\gamma L} \Gamma_L e^{-\gamma L}]^{-1} V(0)$
<p style="text-align: center;">Current transfer function</p> $I(x) = Y_0 [1 - e^{\gamma(x-L)} \Gamma_L e^{\gamma(x-L)}] e^{-\gamma x} [1 - e^{-\gamma L} \Gamma_L e^{-\gamma L}]^{-1} Z_0 I(0)$

## 5. Comparison with Published Experimental and Computer Results

In this section the expressions derived in the paper will be verified and checked with published experimental and computer models for three and four conductor coupled transmission line systems.

### 5.1 Reduction of Inductive Coupling by Reducing Cross-section

In Figure 3 we show a three conductor system consisting of two parallel wires above a ground plane. Consider the coupling from the generator wire 1 to the receptor wire 2. The per-unit-length mutual inductance between the generator circuit and the receptor circuit is related to the cross-sectional area between the receptor wire and the ground plane. This is because the generator circuit produces a magnetic flux, and the mutual inductance is directly related to the portion of this flux which penetrates the area between the receptor wire and the ground plane shown in the shaded region in Figure 3 [5].

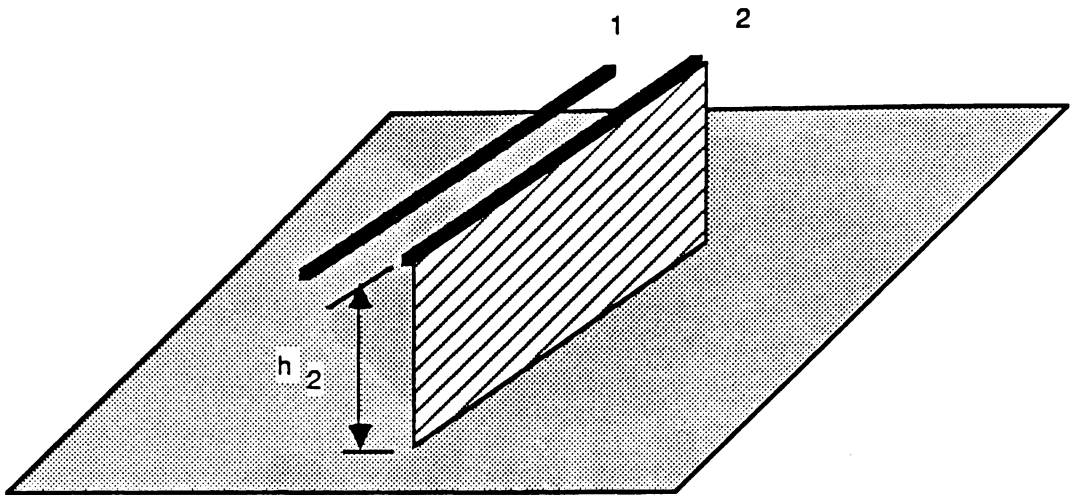


Figure 3 Three conductor system

Now, consider Figure 4 in which a third wire 3 has been added on the receptor side. This wire reduces the cross-section shown in the shaded region which in turn reduces the mutual inductive coupling. Thus, under certain conditions this configuration will result in less coupling than the configuration in Figure 3. Inductive coupling is dominant when the current is large, in other words, when heavy loads are used. Otherwise, capacitive coupling will dominate and the configuration in Figure 4 has no advantage over Figure 3 in terms of reducing coupling. These issues will be investigated using computer programs which calculate the coupled voltage and currents based on the equations derived in this paper.

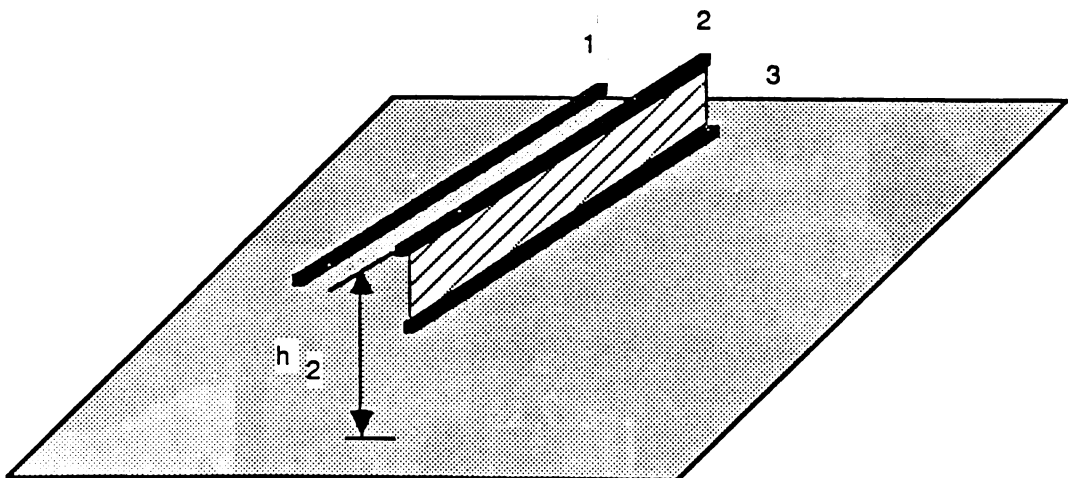


Figure 4. Four conductor system

## 5.2 Four Conductor Transmission Line System

The multiconductor transmission line system to be investigated is shown in Figure 5. In this configuration the coupling between the two straight wires 2 and 3 onto the single wire 1 is of interest. In the following we let,

$$Z_{S11} = 0; Z_{S23} = Z_{L11} = Z_{L23} = R.$$

We are interested in the amount of far-end coupling (voltage across  $Z_{L11}$ ) as the value of  $R$  is changed from 1 Ohm, to 50 Ohms and 1000 Ohms.

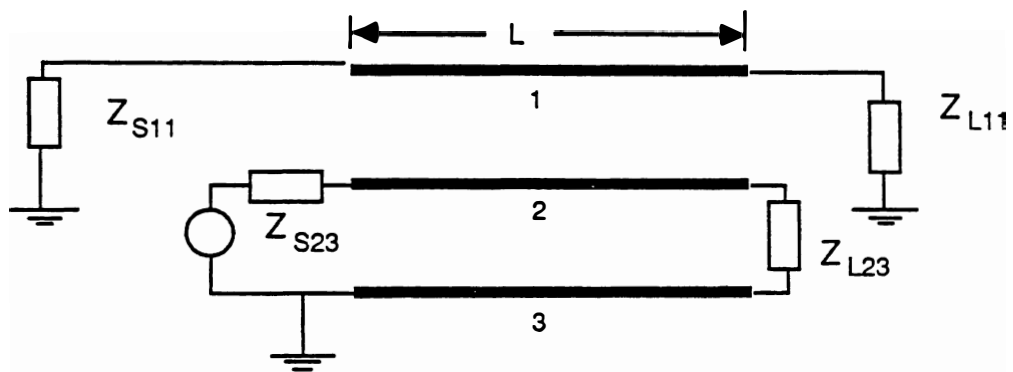


Figure 5. Multiconductor transmission line circuit configuration

The coupling geometry is shown in Figure 6. In the results to follow,

$h = 2 \text{ cm}$ $\Delta h = 0.00166 \text{ m (66 mils)}$ $d = 2 \text{ cm}$ $L = 4.572 \text{ m (15 ft)}$ $r_{w1} = r_{w2} = r_{w3} = 0.406 \text{ mm (16 mils)}$
--

In the above,  $r_{wi}$ ,  $i=1,3$  is the radius of the conductor. The circuit configuration in Figure 5 and the coupling geometry are the same as those in [5] for the case of Straight Wire Pair (SWP) experiments and computer models (the only difference is the length which was 15 ft and 5 1/4 inch



in [5] ). The per unit inductance and capacitance matrix are calculated based on [7]. Losses are taken into account, using a quasi TEM mode approximation.

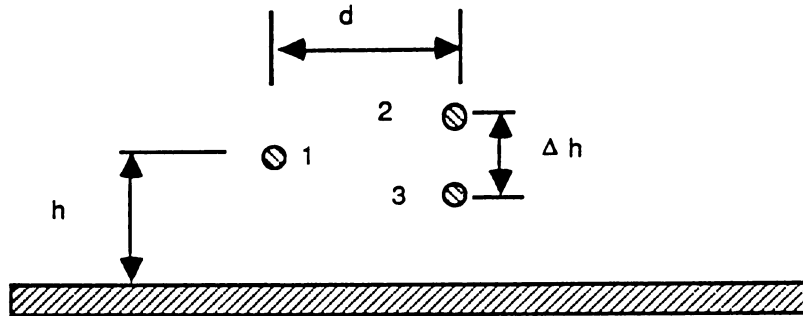


Figure 6. Four conductor coupling geometry

The results of the computer program which evaluates equations (27) for the various values of  $R$  is shown in Figure 7. In the Figure, the far-end crosstalk (voltage across  $Z_{L11}$ ) is plotted against frequency.

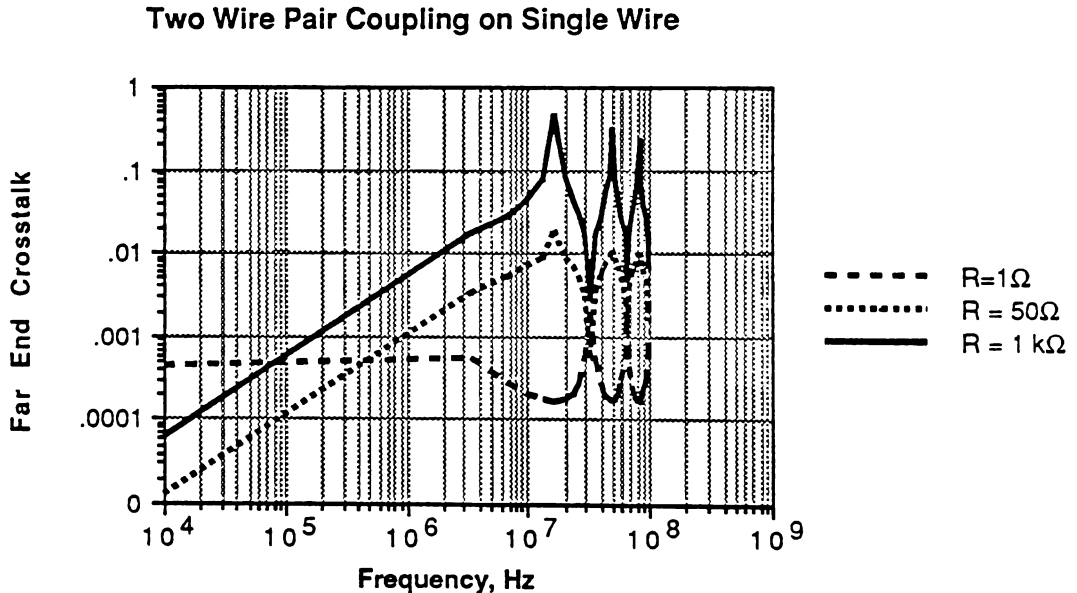


Figure 8. Far-end crosstalk for various loads

An examination of Figure 8 reveals that as the load is increased ( $R$  decreases) the coupling is significantly reduced. This verifies the fact that

the two-wire configuration reduces coupling due to inductive coupling (high currents). As the load is decreased ( $R = 1000$  Ohms) the coupling increases. With this load, the coupling is mainly capacitive and the two-wire configuration has no significant effect in reducing coupling. The results in Figure 8 agree very closely with the experimental and computer models in [5].

### 5.3 Three Conductor Coupling

In the following, a three conductor transmission line system is analyzed. The system consists of two parallel wires above a ground plane. The separation between the wires is 2 cm. Each wire is 2 cm above the ground plane. The wire radius was 0.406 mm (16 mils) for each conductor. The circuit configurations are exactly those of [6]. Specifically, Figure 9 corresponds to example 1, Figure 10 to example 2, and finally Figure 11 to example 3 in [6]. In [6] experimental and theoretical results are presented. The results presented here based on the multiconductor transmission line equations derived in [20] and presented in this paper agree exceptionally well with the experimental results of [6].

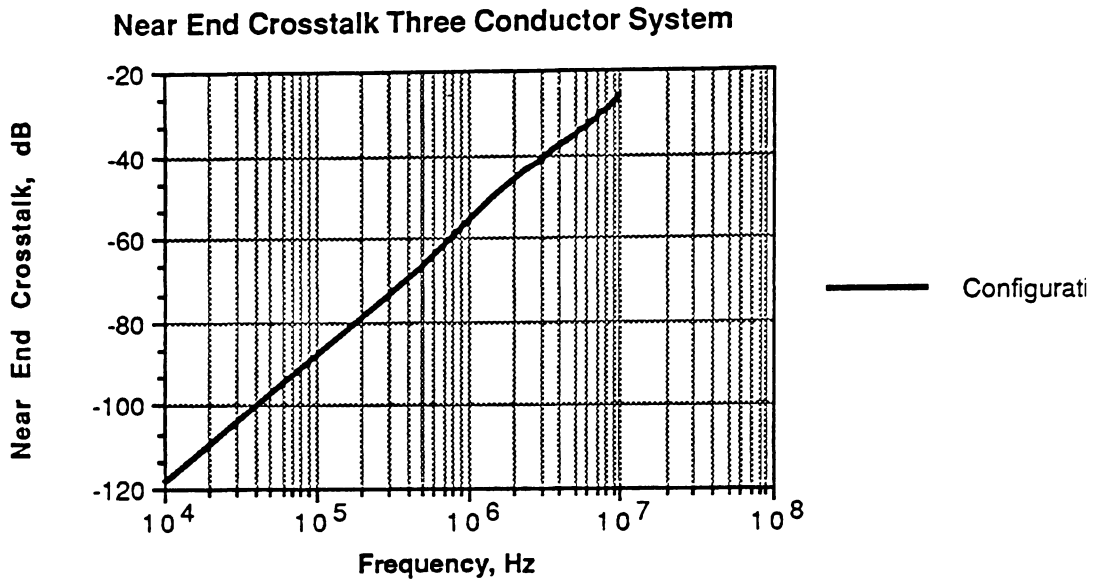


Figure 9 (b).

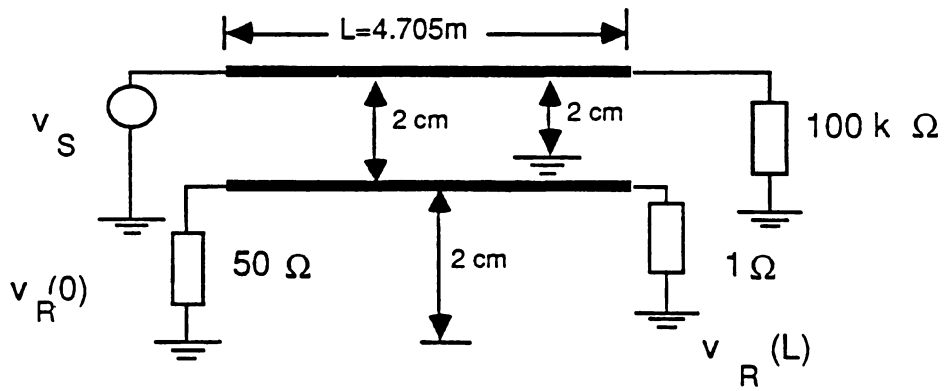


Figure 9(a).

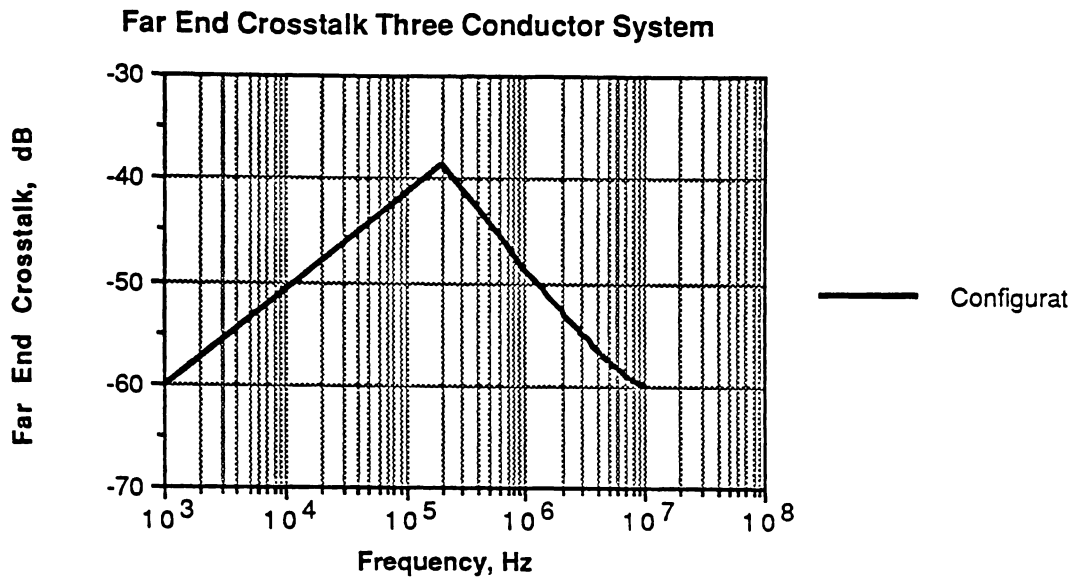


Figure 10(b).

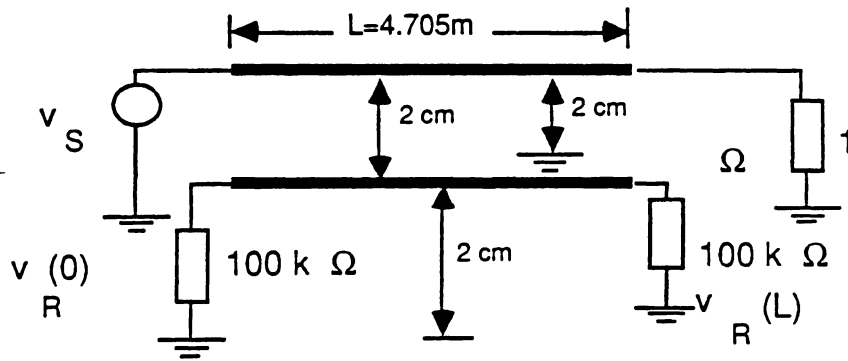


Figure 10(a).

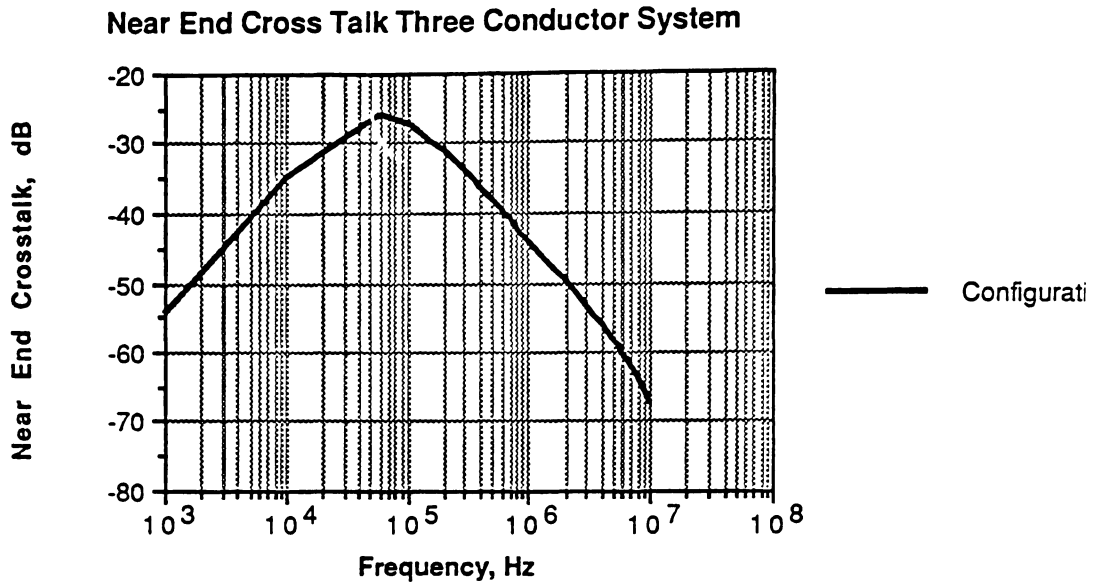


Figure 11 (b).

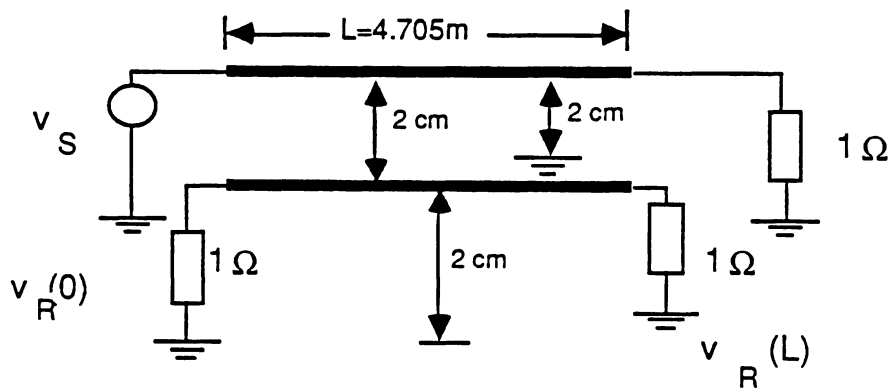


Figure 11(a).

## 6. Conclusions

In this technical report we have presented a derivation of the voltage and current transfer functions of a system of multiconductor transmission lines. The new equations are very compact and suitable for computer modeling of multiconductor transmission line systems with arbitrary loads and sources.

The validity of the derived expressions was verified by comparing results predicted using these equations and published experimental and computer models.

## 7. References

- [1] Lawrence N. Dworsky, *Modern Transmission Line Theory and Applications*, John Wiley and Sons, Inc., 1979.
- [2] Clayton R. Paul, "On uniform multimode transmission lines," *IEEE Trans. on Microwave Theory and Techniques*, August 1973.
- [3] Clayton R. Paul, "Useful matrix chain parameter identities for the analysis of multiconductor transmission lines," *IEEE Trans. on Microwave Theory and Techniques*, Sept. 1975.
- [4] L. M. Gruner, "Multiconductor transmission lines and the Green's matrix," *IEEE Trans. on Microwave Theory and Techniques*, Sept. 1974.
- [5] C. R. Paul, R. J. W. McKnight, "Prediction of Crosstalk Involving Twisted Pairs of Wires -- Part I: A Transmission-Line Model for Twisted-Wire Pairs," *IEEE Trans. on Electromagnetic Compatibility*, Vol. EMC-21, No.2 May 1979.
- [6] C. R. Paul, "On the Superposition of Inductive and Capacitive Coupling in Crosstalk-Prediction Models," *IEEE Trans. on Electromagnetic Compatibility*, Vol. EMC-24, No. 3, August 1982.
- [7] C. R. Paul, "Computation of the Transmission Line Inductance and Capacitance Matrices from the Generalized Capacitance Matrix," *IEEE Trans. on Electromagnetic Compatibility*, Vol. EMC-18, No.4, November 1976.
- [8] V. Belevitch, "Theory of the proximity effect in multiwire cables," Philips Research Reports, Vol. 32, 1977, pp. 16-43

- [9] Robert G. Olsen, "A simple model for weakly coupled lossy transmission lines of finite length," *IEEE Trans. on Electromagnetic Compatibility*, Vol. EMC-26, No. 2, May 1984.
- [10] V. Belevitch and R.R. Wilson, "Cross-Talk in twisted multiwire cables,," *Philips Journal of Research*, Vol. 35, pp 14-58, 1980
- [11] V. Belevitch, "On the theory of cross-talk between twisted pairs," *Philips Research Reports*, Vol. 32, 365-372, 1977.
- [12] V. Belevitch, R. R. Wilson, G. C. Groenendaal, "The capacitance of circuits in a cable with twisted quads," *Philips Research Reports*, Vol. 32, 1977.
- [13] Sasan Ardalán, "CAD of digital communications systems for complex transmission line networks," *National Communications Forum*, Chicago, Ill. Sept. 28-30, 1987
- [14] Sasan Ardalán, "Modeling of complex transmission line systems," *International Workshop on Integrated Electronics and Photonics in Communications*, RTP, N C, Oct. 1987.
- [15] Antonije R. Djordjevic, Tapan K. Sarkar, Roger F. Harrington, "Time-Domain response of multiconductor transmission lines," *Proceedings of the IEEE*, Vo. 75, No. 6, June 1987.
- [16] Mike Riddle, "Modeling Multiple Conductor Transmission Lines," M. Sc. Thesis, Dept. of Electrical and Computer Engineering, North Carolina State University, Sept. 1988.
- [17] John Suh, "Multiconductor Transmission Line Analysis and Measurement," M. Sc. Thesis, Dept. of Electrical and Computer Engineering, North Carolina State University, May 1988.